THE JOURNAL OF PHYSICAL CHEMISTRY LETTERS
A JOURNAL OF THE AMERICAN CHEMICAL SOCIETY

pubs.acs.org/JPCL

Letter

Measuring the Electric Fields of Ions Captured in Crown Ethers

Anwesha Maitra, William R. Lake, Ahmed Mohamed, Sean C. Edington, Pratyusha Das, Barry C. Thompson, Sharon Hammes-Schiffer, Mark Johnson, and Jahan M. Dawlaty*

Cite This: *J. Phys. Chem. Lett.* 2024, 15, 7458−7465

Read Online

ACCESS | Metrics & More | Article Recommendations | Supporting Information

ABSTRACT: Controlling reactivity with electric fields is a persistent challenge in chemistry. One approach is to tether ions at well-defined locations near a reactive center. To quantify fields arising from ions, we report crown ethers that capture metal cations as field sources and a covalently bound vibrational Stark shift probe as a field sensor. We use experiments and computations in both the gas and liquid phases to quantify the vibrational frequencies of the probe and estimate the electric fields from the captured ions. Cations, in general, blue shift the probe frequency, with effective fields estimated to vary in the range of ∼0.2−3 V/nm in the liquid phase. Comparison of the gas and liquid phase data provides insight into the effects of mutual polarization of the molecule and solvent and screening of the ion's field. These findings reveal the roles of charge, local screening, and geometry in the design of tailored electric fields.

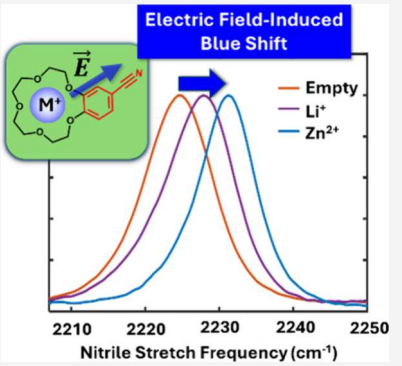

Electric fields experienced by a molecule arise from orientation of solvent dipoles, organization of ions, and the presence of nearby polarizable entities. Such fields influence the thermodynamics and kinetics of a vast range of reactions, especially if the reactants, products, or transition states are charged or dipolar. The magnitude and direction of such fields are a natural consequence of the molecular electrostatic environment. To control and direct chemical reactions, it is often necessary to tailor the local electrostatics. Such engineering of the chemical microenvironment is an important frontier of contemporary chemistry.

The effects of electric fields on reactions are manifested in a variety of scenarios, especially in electrochemical, molecular, and enzymatic catalysis. Two examples are the through-space substitution effect on iron(0) tetraphenylporphyrins to catalyze electrochemical conversion[1] of CO_2 to CO and the electron-catalyzed dehydrogenation reaction of ethylene.[2] In addition, Surendranath and co-workers have shown that spontaneous electric fields generated by interfacial proton and electron transfer in different solvents can affect hydrogenation reactions on a Pt/C catalyst.[3] Similarly, polarizing fields emanating from charged entities, such as titratable amino acids, in an enzyme[4−6] also influence chemical reactions. Furthermore, a number of studies have shown that installing a charge at well-defined locations relative to a reactive center can control the reaction mechanisms and selectivity of molecular catalysts.[7−11]

The influence of these electric fields on reactions can be due to a number of factors, including preorganization, electrostatic attraction or repulsion in bimolecular reactions, and direct polarization of a chemical bond.[12−17] For example, the presence of a potassium ion in the deacetylase active site helps preorganize the residues to activate the protein function,[12] whereas the presence of higher cationic charges can reduce the rate of N_2 formation in bimolecular coupling reactions.[15] As another example, the presence of cationic charge in a copper catalyst was shown to affect C−H activation by polarizing the C−H bond.[14] Electric fields from ions can also affect excited states and photodissociation reactions.[18] Therefore, it is important to quantify the localized electric fields emanating from ions more systematically at molecular length scales.

Inspired by the work by Yang and co-workers,[15,19,20] we have designed a model molecule that aids in quantifying the electric fields emanating from cations. Our molecule is a crown ether that bears a covalently attached benzonitrile (Figure 1a,b), which is a known vibrational probe for sensing local electric fields.[21−27] The probe, which resides within a nanometer of the captured ion, reports the effective electric field from the cation. We present vibrational spectroscopy results in the liquid phase for the crown ethers loaded with a number of cations with 1+, 2+, and 3+ charges. To better isolate the effects of solvent and counterions and to understand the geometry of the cations in the crown, we also report vibrational spectra in the gas phase. Finally, with support from computational work, we describe the factors that affect the electric fields generated by the ions and sensed by the probe.

Received: May 3, 2024
Revised: July 10, 2024
Accepted: July 11, 2024
Published: July 15, 2024

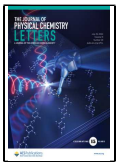

https://doi.org/10.1021/acs.jpclett.4c01303
J. Phys. Chem. Lett. 2024, 15, 7458−7465

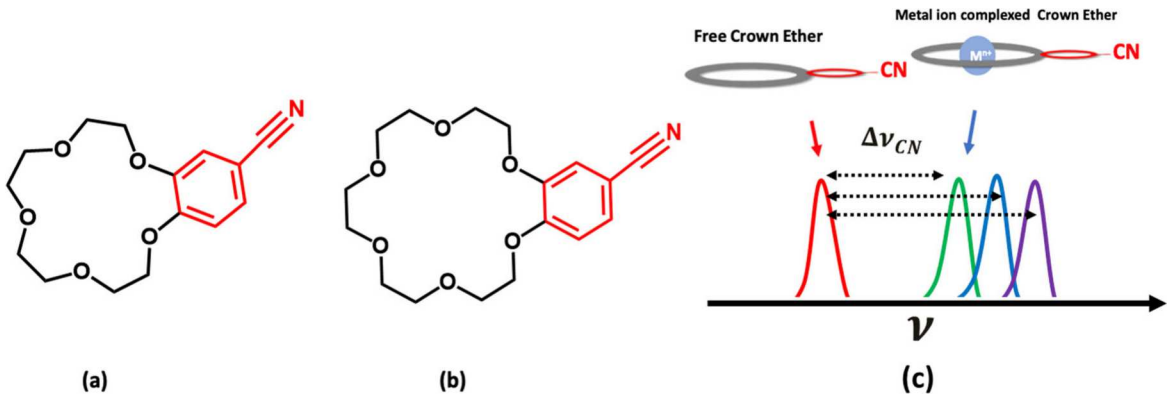

Figure 1. Synthesized crown ethers with benzonitrile vibrational probe. (a) benzo-15-crown-5-CN (B-15C5-CN). (b) benzo-18-crown-6-CN. (c) Cartoon of expected blue-shift of CN frequency after capturing a metal ion (M^{n+}).

All reactions were carried out under dry N_2 in oven-dried glassware, unless otherwise noted. Anhydrous dichloromethane (DCM) (Sigma- Aldrich), Acetonitrile (EMD), tetraethylene glycol (Sigma-Aldrich), pentaethylene glycol (Sigma-Aldrich), p-toluenesulfonyl chloride (TsCl) (Alfa Aesar), and 3,4-dihydroxybenzonitrile (Sigma-Aldrich) were purchased and used as received. Potassium carbonate (K_2CO_3) was dried at 120 °C in a vacuum oven overnight prior to use. Crown ethers B15C5-CN and B18C6-CN were prepared according to literature procedure.[28] Details of the reaction schemes, synthesis of the tosylate precursors and crown ethers, and NMR characterizations can be found in the Supporting Information.

The FT-IR spectra were recorded for 400 mM of crown ethers with and without various metal salts in a Thermo Scientific Nicolet iS50 spectrometer. A demountable FT-IR cell from International Crystal Laboratories was used to hold two calcium fluoride windows separated by a 15 μm Teflon spacer, and FT-IR spectra were acquired in transmission mode with a liquid nitrogen cooled MCT detector. Highly polar propylene carbonate (dielectric constant: 64.9) was used as solvent, as this can dissolve all the metal salts and the crown ethers. Spectra for the metal ions complexed with crown ethers were obtained using 1:1 mixtures of metal salts and crown ethers. Our estimated error in assigning frequencies is ±0.25 cm^{-1} arising from 0.5 cm^{-1} resolution of the instrument. The salts were used as purchased from Sigma-Aldrich. Trifluoromethanesulfonate (OTf^-, $[CF_3SO_3]^-$) and bis(trifluoromethane)sulfonimide ($TFSI^-$, $[(CF_3SO_2)_2N]^-$) were used as counteranions. The OTf^- and $TFSI^-$ anions are larger in size, and they can remain dissociated from the metal ions. The metal salts used in this work are LiTFSI, NaTFSI, KOTf, $Mg(TFSI)_2$, $Ca(OTf)_2$, $Ba(OTf)_2$, $Zn(TFSI)_2$, $Mn(OTf)_2$, $Ni(OTf)_2$, $Cu(OTf)_2$, $Al(OTf)_3$, $Sc(OTf)_3$, $Eu(OTf)_3$, $Y(OTf)_3$, $Yb(OTf)_3$, and $In(OTf)_3$. The spectra were baseline corrected.

The gas-phase spectra presented here were recorded using a custom-built, tandem photofragmentation mass spectrometer, which has been described in detail previously.[29] In short, the crown ether complexes were extracted from solution and ionized using electrospray ionization (ESI). The ions so produced were introduced into vacuum through multiple stages of differential pumping and held in a cryogenically cooled, radio frequency Paul trap, where they were cooled to ~20 K through collisions with helium buffer gas. The buffer gas was doped with 10% D_2, which was employed as a mass tag. At the cryogenic temperatures maintained in the ion trap, the D_2 mass tag forms a weakly bound complex with the ion under study. Infrared spectra were recorded by scanning a pulsed laser (Laser Vision, 10 mJ, 10 ns, 10 Hz repetition rate) over the reported frequency range. When the laser pulse is resonant with a vibrational mode of the ion under study, absorption of a single photon is sufficient to effect photodissociation of the mass tag through intramolecular vibrational redistribution. Monitoring photofragmentation of the weakly bound complex as a function of laser frequency thus yields infrared action spectra in a linear, single-photon regime.

We used the Conformer-Rotamer Ensemble Sampling Tool (CREST)[30,31] to perform a conformational search on the B15C5-CN crown ether with 13 different metal ions (Cs^+, K^+, Li^+, Na^+, Rb^+, Ba^{2+}, Be^{2+}, Ca^{2+}, Mg^{2+}, Sr^{2+}, Zn^{2+}, Al^{3+}, and Sc^{3+}). In total, this procedure identified 542 local minima at the density functional tight binding (DFTB) level of theory across all ions. Further details on the CREST conformational search can be found in the SI. These 542 different configurations were then used as starting geometries for density functional theory (DFT) geometry optimizations using the B3LYP[32] functional with Grimme's D3[33] dispersion correction, in conjunction with the 6-31++G** basis set[34−39] for all atoms except the ions and the LANL2DZ[40−42] basis set, which has an effective core potential, for the ions. These geometry optimizations were performed in the gas phase. After these DFT geometry optimizations, the total number of distinct configurations was reduced to 225 due to some redundancies. The number of distinct configurations for each ion varied from 43 for Li^+ to 1 for Ba^{2+}. For each ion, harmonic vibrational frequencies were computed for the three lowest-energy optimized structures in the gas phase. Additionally, for each ion, we reoptimized those three structures and calculated the harmonic vibrational frequencies with implicit solvent using the conductor-like polarizable continuum model (C-PCM)[43−45] with a dielectric constant of 64.9 for propylene carbonate, including the nonelectrostatic contributions of dispersion, repulsion, and cavitation energies.[43,44] The solution phase calculations did not include the counterions. For Ba^{2+}, Be^{2+}, and Ca^{2+}, fewer than three distinct optimized structures were found within 1 kcal/mol of the minimum energy structure in the gas phase, so only one (for Ba^{2+}) or two (for Be^{2+} and Ca^{2+}) structures were analyzed in this manner. The vibrational frequencies for the ion-free structure were obtained by removing the ion from the lowest-energy Li^+ structure, optimizing the geometry, and performing a harmonic

https://doi.org/10.1021/acs.jpclett.4c01303
J. Phys. Chem. Lett. 2024, 15, 7458−7465

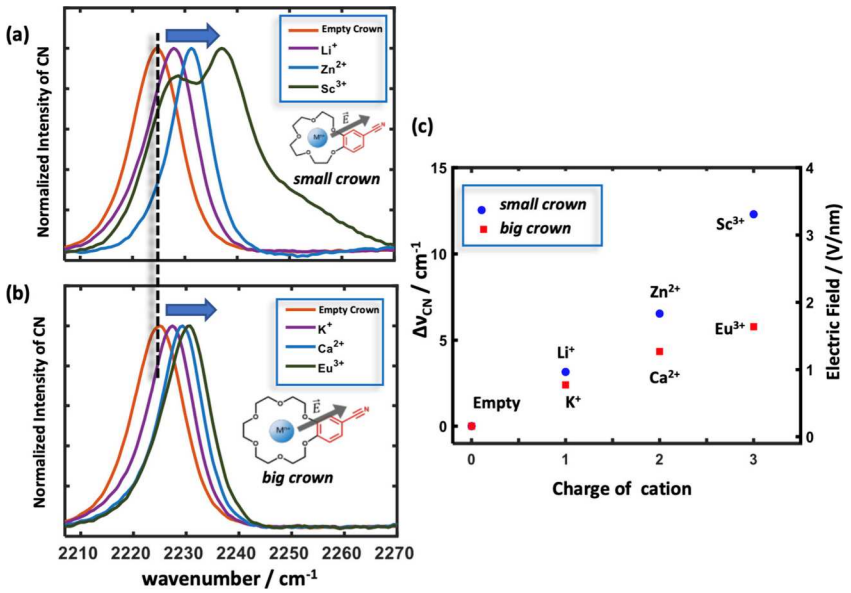

Figure 2. (a) IR absorption spectra of cation-complexed benzo-15-crown-5-CN and (b) benzo-18-crown-6-CN in propylene carbonate for the ions indicated. (c) Maximum CN frequency shifts obtained for benzo-15-crown-5-CN (blue circles) and benzo-18-crown-6-CN (red squares) among the cations studied for each charge.

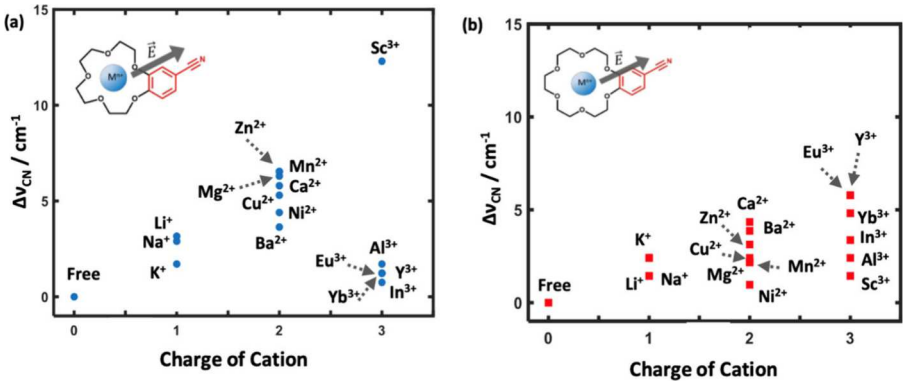

Figure 3. CN frequency shift in propylene carbonate versus charge of cation complexed with (a) benzo-15-crown-5-CN (small crown) or (b) benzo-18-crown-6-CN (big crown). Significant differences in frequencies are observed for cations of the same charge.

vibrational frequency analysis. All of these DFT calculations were performed with the Gaussian16 software package.[46]

We used 16 cations of charges 1+, 2+, and 3+ in this study. For simplicity, first it is useful to only plot the cations that produced the largest shifts for their charge. The IR spectra in the nitrile range of the two crown ethers bearing these cations are shown in Figure 2a,b. The figures show that the frequencies of the ion-free crown ethers for the small and large crowns are nearly identical (2225 cm^{-1}). As cations are inserted in the crowns, the CN frequency blue shifts as expected for a field emanating from the cation. The ratio of metal ion to crown ether was 1:1 in all of these measurements, except for Sc^{3+}, where a higher ratio of 2:1 was used due to the smaller affinity of Sc^{3+} for the crown ether. Even at this ratio, only partial occupancy was achieved, as evidenced by the two peaks in the spectrum (Figure 2a).

The frequency shifts relative to free crown ether are summarized in Figure 2c, which shows that more highly charged ions produce larger shifts in both crowns. However, the frequency shift is more sensitive to charge for the smaller crown. Although the field from the cation is expected to be inhomogeneous across the body of the benzonitrile probe, it is still useful to estimate the approximate or effective value of this field from the known Stark tuning rate of the benzonitrile molecule (~3.6 cm^{-1}/V/nm).[47] The right vertical axis in Figure 2c shows this effective field change felt by the nitrile, which varies from ~0.5−3 V/nm.

We also observed IR peaks that were blue-shifted by a very large amount (40−50 cm^{-1}) for some of the cations (e.g., Zn^{2+}, Cu^{2+}, and Y^{3+}). These spectra are shown in the SI Figure S5 and do not arise from the Stark effect of the cation, but rather from direct Lewis coordination of the nitrile lone pair with the cations, as reported previously.[48] Similar effects have been observed for acetonitrile in previous work.[49] Such peaks also arise when the cations are placed in pure benzonitrile. Since these peaks do not arise from the electrostatic influence of the captured ions, they are not the subject of this study.

The data for all of the studied cations is shown in Figure 3, which exhibits a range in the frequency shift induced by cations of the same charge. For the smaller crown ether (Figure 3a), the shift produced by Li^+ is larger than that of K^+, even though they both have the same charge. Similarly, a range of shifts is observed for the doubly charged cations. For the triply charged cations complexed in the smaller crown ether, most of them

https://doi.org/10.1021/acs.jpclett.4c01303
J. Phys. Chem. Lett. 2024, 15, 7458−7465

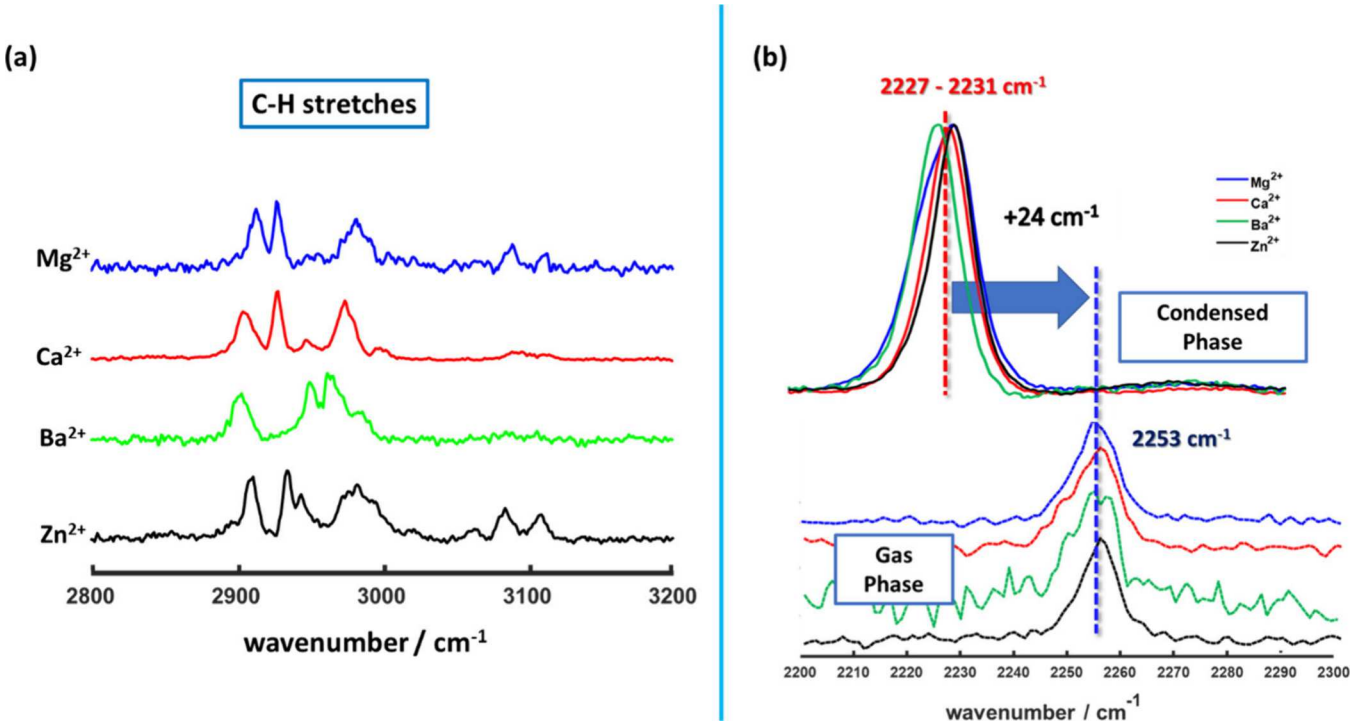

Figure 4. (a) CH stretching frequencies in gas phase experiment for M^{2+} complexes with benzo-15-crown-5-CN (smaller crown) indicating different coordination geometries and (b) CN stretching frequencies for M^{2+} complexes with benzo-15-crown-5-CN (smaller crown) in liquid phase (top) and in gas phase (bottom).

induce either a small shift or no shift at all, with the exception of Sc^{3+}. The larger crown ether exhibits a range of frequency shifts as well, with the triply charged cations behaving more similarly to the doubly charged cations. As discussed below, the frequency shift in the absence of solvent is much greater than these variations. Understanding the details of these smaller differences in the nitrile vibrational frequency for ions with the same charge in the complex solvent and counterion environment is beyond the scope of this work.

The results presented above strongly suggest that a number of factors, including complexation geometries, solvent effects, and counterions, affect the electric field experienced by the probe. In the liquid phase, it is impossible to cleanly isolate these effects. Therefore, we turned to low temperature gas phase ion spectroscopy, which allows us to isolate the spectrum of a crown-ion complex without the involvement of solvent and counterions. This approach is a powerful tool for discerning the inherent field produced by the ion, and in conjunction with the liquid phase data can reveal the net influence of solvent and counterion screening.

Representative gas phase spectra in the CN stretch region for the small crown complexes with 2+ ions (Mg^{2+}, Zn^{2+}, Ca^{2+}, Ba^{2+}) are shown in Figure 4b. The corresponding CH stretch spectra for these 2+ ions are shown in Figure 4a. Even though all these ions carry the same charge, there are distinct variations in the CH stretch frequencies. There are five peaks in the aliphatic CH stretch region, as distinctly observed for the Ca^{2+} complex. The frequencies of these peaks vary significantly for the other complexes (see SI), indicating that their coordination geometries to the crown are different. However, interestingly, the nitrile frequencies for all of these complexes are nearly identical (2253 cm^{-1}) and largely blue-shifted (~+24 cm^{-1}) compared to the liquid phase values (Figure 4b).

The CN stretch was too weak to be observed for the 1+ ion complexes. We could observe the gas phase spectrum of one 3+ ion (Eu^{3+}), which had a complex structure indicating several coordination geometries, including direct coordination of the ion with the nitrile probe. Since these peaks do not uniquely report on the electrostatic effects, which is the focus of this work, we did not perform further analysis.

To further elucidate the CN frequencies in the gas phase and in the liquid phase, we analyzed the CN frequencies for the smaller crown ether computed with DFT. For each cation, we computed the average of the nitrile vibrational frequencies for the three lowest-energy optimized geometries, with the exceptions discussed above. These results are shown in Figure 5, and the calculated frequencies are given in Tables S1 and S2. The average difference between the CN vibrational frequency in solvent versus gas phase across all ions is 22 cm^{-1}. The optimized geometries of the crown ethers vary widely, even with the same ions complexed in the crown, mainly because the ethyl groups that comprise the crown are very flexible. Nevertheless, the nitrile vibrational frequency for a given cation rarely changes by more than 1 cm^{-1} for the three lowest-energy geometries. This observation can be partially explained by the consistent geometric relationship between the ion and the nitrile group for the three lowest-energy geometries with the same ion. The distance from the midpoint of the nitrile bond to the ion varies with ion identity, from 7.0 Å for Be^{2+} to 8.2 Å for Rb^{+}. The angle defined by the ion, nitrile carbon, and nitrile nitrogen (XCN angle) is ~160° with a range between 150° and 162°. The lowest-energy structure for each ion is shown in Figure 6. Note that our conformational search was not exhaustive, and other low energy structures are possible. The most important finding from these DFT calculations is that the nitrile frequency is significantly different when the molecule is in the liquid phase

https://doi.org/10.1021/acs.jpclett.4c01303
J. Phys. Chem. Lett. 2024, 15, 7458−7465

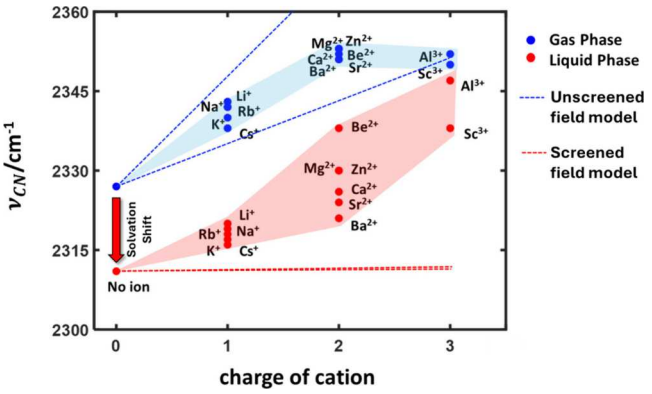

Figure 5. Computed CN vibrational frequency shift for different cations complexed to benzo-15-crown-5-CN (smaller crown) in the gas phase (blue) and in the liquid phase (red). Each data point corresponds to a different cation and is averaged over up to three different optimized geometries. Note that some data points are not visible because of overlap. The charges of the cations computed with the natural bond orbital analysis are provided in Table S3. The dashed lines represent the frequency change based on a linear Stark shift and a simple electrostatic view of fields (blue ϵ_r = 1, red ϵ_r = 64.9). For each case, two lines are drawn for electric fields due to a cation at a distance of 0.5 nm (top, higher slope) or 0.8 nm (bottom, smaller slope) from the probe. The red lines have very shallow slopes because of the large dielectric screening, revealing clear deviation of the data from the simple screened model of the field.

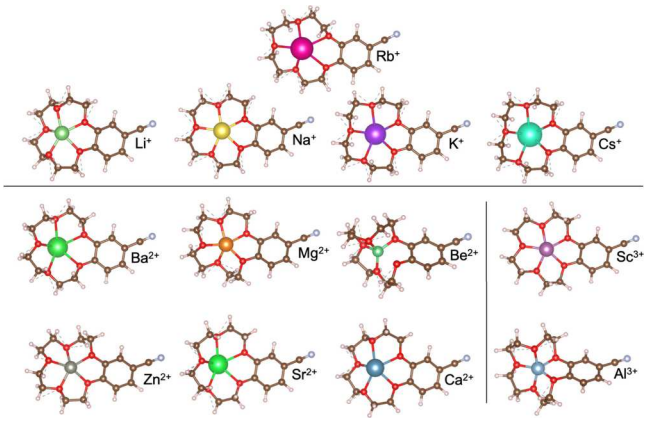

Figure 6. Calculated minimum energy geometries for the small crown ether with each ion bound. Atoms are brown for carbon, light blue for nitrogen, red for oxygen, and white for hydrogen. The colorful central atom in each structure is the metal ion.

versus the gas phase. The calculated changes in the electron density upon solvation, as well as the changes in the occupancy of the nitrile bonding and antibonding orbitals computed using a natural bond orbital analysis,[50−55] indicate that solvation increases the electron density on the nitrile (Figure S8 and Table S4). Moreover, the additional electron density on the nitrile for the ion free and +1 and +2 cationic systems preferentially occupies the antibonding orbital, thereby weakening the CN bond and decreasing the frequency. These effects are presumably due to the mutual polarization of the molecule and solvent but are quite subtle and may depend on the level of theory.

From the combination of experimental and computational work, we draw the following conclusions. First, both the experimental spectra in Figure 4b and the computational data in Figure 5 show a large shift between the gas phase and the liquid phase frequencies for the 2+ cations. The computational data exhibit a shift of approximately 22 cm^{-1} between the average value of the liquid phase and gas phase frequencies, which is in reasonable agreement with the 24 cm^{-1} observed experimentally (Figure 4). Note that for the computed frequencies, even in the absence of ions, a significant shift of 16 cm^{-1} exists between the gas phase and liquid phase values. Therefore, a significant contribution to the 22 cm^{-1} shift for the 2+ cations arises from the solvation of the crown and the nitrile even if the ion is not present. The solvent screens the charge of the cation, which also partially contributes to the 22 cm^{-1} difference between the gas phase and liquid phase values. However, we caution that the two solvent effects on frequency, namely those arising from solvation of the molecule and from screening of the ion, may not be viewed as additive. In our work, when comparing the gas and liquid phase frequencies for the 2+ ion bearing crowns, the solvent acts on both the molecule and the ion at the same time, and therefore a precise dissection of the various contributions is not possible.

Next, we compare the observed frequency shifts with the expectations from a simple electrostatic view of fields in a continuum medium. The magnitude of an electric field at a distance r from a charge q in a medium of dielectric constant ϵ_r is $E = q/(4\pi\epsilon_0\epsilon_r r^2)$. For benzonitrile, the field can be related to the frequency shift within the linear Stark shift approximation as $\upsilon = \upsilon_0 + \Delta\mu E$, where the Stark tuning rate $\Delta\mu \approx 3.6\ \text{cm}^{-1}/\left(\frac{\text{V}}{\text{nm}}\right)$ for benzonitrile.[47] Therefore, setting υ_0 as the frequency in the absence of ions, the frequency υ is expected to change linearly as q increases with a slope determined by the distance r and dielectric constant ϵ_r. The dashed lines in Figure 5 represent the expected change in frequency based on this model for the probe at two representative distances of r = 0.5 nm and r = 0.8 nm from the cation. The two blue dotted lines for the gas phase (ϵ_r = 1) bracket the computational data reasonably well. The deviation of the last data points for 3+ cations may be attributable to the departure of the Stark response from linearity at large field values.[47] The slopes of the red dashed lines for the liquid phase are naturally smaller than those of the gas phase by a factor of ϵ_r = 64.9 and imply that in the liquid phase, screening is so strong that the presence of the cation, as well as changing its charge, should not change the frequency appreciably. However, both the computational data in Figure 5 and the experimental data in Figure 3 show that the frequencies do have significant shifts upon addition of cations and changing the cation charge. Therefore, the simple model of the field and dielectric screening as noted above is inadequate to describe the field-induced frequency changes in the liquid phase. Interestingly, the frequency shift as a function of cation charge is present both in the experiments with real solvents and in computations with a dielectric continuum solvent. This implies that the net influence of the charge on the probe in the liquid phase is significant but not sensitive to the molecular structure of the solvent or the counterions. The likely origin of this effect is that the geometry of the ion relative to the plane of the benzonitrile is such that the cation directly influences the benzonitrile probe without intervening solvent (Figure 6), and screening by the solvent above and below the plane is relatively small.

An important consequence of this observation for engineering fields on the molecular level is that even in high dielectric media, the field values near charged ions and at molecular

https://doi.org/10.1021/acs.jpclett.4c01303
J. Phys. Chem. Lett. 2024, 15, 7458−7465

length scales can be much higher than implied by the dielectric constant. One may be tempted to interpret the observed shifts as if the medium effectively has a reduced dielectric constant. Given the spread in the data, and the nuances of the screening on the molecular scale, we caution that such a view may be oversimplified. Further, the field is inhomogeneous around the ion, and the Stark response may also deviate from linearity at large values. Coordination of the solvent to the ion and dielectric saturation very close to the ion may not be captured by a continuum model. We have examined a few explicit solvent interactions with the crown (see SI). Full exploration of the solvent geometries is beyond the scope of this work.

In summary, we have addressed the electrostatics of a complex and chemically relevant environment with a multipronged approach that combines results from liquid phase and gas phase both experimentally and computationally. Our novel concept of tethering a Stark probe near an ion captured in a crown ether and synthesis of molecules with two different cavity sizes enabled us to examine a large number of ions in those cavities. This way of measuring electric fields from a single ion in a chemically relevant environment with a well-defined probe has not been attempted before. The crown motifs have been used in organometallic complexes for controlling the reactivity of nearby catalytic centers.[19,20] Our work can therefore help guide the design principles for such motifs since we have quantified the otherwise hard to measure local electric field and solvent screening on the molecular scale.

Below we outline three most important outcomes of our work that are relevant for using oriented fields in catalysis. The first outcome is that even in the liquid phase and in the presence of a high dielectric solvent, the ions within the crown can induce a vibrational Stark effect, and thereby can polarize an appropriately positioned molecule. From a simple electrostatic view, a high dielectric constant solvent such as propylene carbonate, with ϵ_r = 64.9, should attenuate the field from the ion by a large amount relative to vacuum, rendering it effectively unusable. However, our experimental and computational data show that the Stark probe responds to the presence of the cation and changes of its charge both in vacuum and in the liquid phase. Therefore, using a simple electrostatic model to estimate the screening of the charge within a crown complex is not appropriate. The reason may lie in the geometry of the ion relative to the Stark probe, which does not allow intervening solvent between the probe and the ion.

The second outcome of the work is revealing the full range of tunability of fields that can be afforded by the choice of 1+, 2+, and 3+ ions in the liquid phase. We report that the observed range of frequency shifts in the liquid phase (∼1−12 cm^{-1}) is only somewhat larger than the response of benzonitrile in a dielectric series of solvents (∼7 cm^{-1}) mentioned above.[25,56] This does not take away from the utility of the crown concept in controlling the local electrostatics in the liquid phase. Even though many of the ions induce a field that is comparable to the solvation field of a high-dielectric solvent, it should be borne in mind that the field from the ion is directional and controllable. A solvent field, on the other hand, is created by the overall structure of the solvent, which is often difficult to precisely control and direct. An ion in a crown ether, even if it exerts a field of similar magnitude to that of a solvent cavity, can do so in a directional way. Furthermore, independent of the rest of the system, the crown concept allows a palette of choices for ions for tuning the field required for desired applications.

The third unexpected outcome of the work is that in the liquid phase we observed variations in the frequency of the probe even for ions of the same charge. In contrast, in the gas phase there is no discernible variation in the probe frequency for ions of the same charge. Interestingly, our computational results in a continuum dielectric also reveals a larger range of variation compared to the computations in the vacuum for 2+ ions. This observation shows that precise control of local electric fields in the condensed phase is not merely a matter of placing a charge at a specific distance. The solvent, and surprisingly even when the solvent is treated in the computations as a dielectric continuum, results in significant variations in the induced field. Such variations may be correlated with changes in the geometries of ion coordination that are also revealed by our computations.

Finally, controlling electrostatics with ions, and in particular ions captured in crown ethers, is gaining popularity in catalysis. Our paper quantifies the values of fields, explores the limits, and highlights the complexities that need to be addressed when engineering directed electric fields in the liquid phase. Motifs with multiple well-placed ions for more detailed control of the electrostatics of a reactive center are at the frontiers of research. Exploring chemical reactivity in such electrostatically engineered environments, while maintaining optimal transport and sterics of the reactive center, is a major challenge for contemporary efforts in catalyst design.

■ ASSOCIATED CONTENT

Supporting Information

The Supporting Information is available free of charge at https://pubs.acs.org/doi/10.1021/acs.jpclett.4c01303.

Details of the synthesis of the crown ethers, NMR characterizations, liquid phase IR spectra data analysis, representative spectra, CREST conformation search, computed harmonic vibrational frequencies, explicit solvent test (PDF)

■ AUTHOR INFORMATION

Corresponding Author

Jahan M. Dawlaty − *Department of Chemistry, University of Southern California, Los Angeles, California 90089, United States;* orcid.org/0000-0001-5218-847X; Email: dawlaty@usc.edu

Authors

Anwesha Maitra − *Department of Chemistry, University of Southern California, Los Angeles, California 90089, United States*

William R. Lake − *Department of Chemistry, Yale University, New Haven, Connecticut 06520, United States;* orcid.org/0000-0001-8182-3583

Ahmed Mohamed − *Department of Chemistry, Yale University, New Haven, Connecticut 06520, United States*

Sean C. Edington − *Department of Molecular, Cellular, and Biomedical Sciences and Department of Chemistry, University of New Hampshire, Durham, New Hampshire 03824, United States;* orcid.org/0000-0002-5894-8801

Pratyusha Das − *Department of Chemistry, University of Southern California, Los Angeles, California 90089, United States*

Barry C. Thompson − *Department of Chemistry and Loker Hydrocarbon Institute, University of Southern California, Los*

https://doi.org/10.1021/acs.jpclett.4c01303
J. Phys. Chem. Lett. 2024, 15, 7458−7465

Angeles, California 90089, United States; orcid.org/0000-0002-3127-0412

Sharon Hammes-Schiffer − *Department of Chemistry, Princeton University, Princeton, New Jersey 08544, United States;* orcid.org/0000-0002-3782-6995

Mark Johnson − *Department of Chemistry, Yale University, New Haven, Connecticut 06520, United States;* orcid.org/0000-0002-1492-6993

Complete contact information is available at: https://pubs.acs.org/10.1021/acs.jpclett.4c01303

Notes

The authors declare no competing financial interest.

■ ACKNOWLEDGMENTS

The work was supported by the Air Force Office of Scientific Research AFOSR award FA9550-21-1-0170 and FA9550-18-1-0420. J.M.D. was partially supported by the grant CHE 2154493 from the National Science Foundation (NSF). W.L. and A.M. were partially supported by the Air Force Office of Scientific Research AFOSR award FA9550-18-1-0420 (S.H.-S. and J.M.D.) A.M. was partially supported by the Air Force Office of Scientific Research AFOSR award FA9550-18-1-0213 in the context of metal interactions with organic ionophores for the purpose of small molecule activation.

■ REFERENCES

(1) Azcarate, I.; Costentin, C.; Robert, M.; Savéant, J.-M. Through-space charge interaction substituent effects in molecular catalysis leading to the design of the most efficient catalyst of CO_2-to-CO electrochemical conversion. *J. Am. Chem. Soc.* **2016**, *138*, 16639−16644.

(2) Chen, H.; Jiang, F.; Hu, C.; Jiao, Y.; Chen, S.; Qiu, Y.; Zhou, P.; Zhang, L.; Cai, K.; Song, B.; et al. Electron-catalyzed dehydrogenation in a single-molecule junction. *J. Am. Chem. Soc.* **2021**, *143*, 8476−8487.

(3) Wesley, T. S.; Román-Leshkov, Y.; Surendranath, Y. Spontaneous electric fields play a key role in thermochemical catalysis at metal−liquid interfaces. *ACS Cent. Sci.* **2021**, *7*, 1045−1055.

(4) Ondrechen, M. J.; Briggs, J. M.; McCammon, J. A. A model for enzyme−substrate interaction in alanine racemase. *J. Am. Chem. Soc.* **2001**, *123*, 2830−2834.

(5) Sissi, C.; Palumbo, M. Effects of magnesium and related divalent metal ions in topoisomerase structure and function. *Nucleic Acids Res.* **2009**, *37*, 702−11.

(6) Fried, S. D.; Bagchi, S.; Boxer, S. G. Extreme electric fields power catalysis in the active site of ketosteroid isomerase. *Science* **2014**, *346*, 1510−1514.

(7) Shaik, S.; de Visser, S. P.; Kumar, D. External electric field will control the selectivity of enzymatic-like bond activations. *J. Am. Chem. Soc.* **2004**, *126*, 11746−11749.

(8) Shaik, S.; Ramanan, R.; Danovich, D.; Mandal, D. Structure and reactivity/selectivity control by oriented-external electric fields. *Chem. Soc. Rev.* **2018**, *47*, 5125−5145.

(9) Yue, L.; Wang, N.; Zhou, S.; Sun, X.; Schlangen, M.; Schwarz, H. The electric field as a "smart" ligand in controlling the thermal activation of methane and molecular hydrogen. *Angew. Chem., Int. Ed.* **2018**, *57*, 14635−14639.

(10) Shaik, S.; Danovich, D.; Joy, J.; Wang, Z.; Stuyver, T. Electric-field mediated chemistry: Uncovering and exploiting the potential of (oriented) electric fields to exert chemical catalysis and reaction control. *J. Am. Chem. Soc.* **2020**, *142*, 12551−12562.

(11) Siddiqui, S. A.; Dubey, K. D. Can the local electric field be a descriptor of catalytic activity? A case study on chorismate mutase. *Phys. Chem. Chem. Phys.* **2022**, *24*, 1974−1981.

(12) Nechay, M. R.; Gallup, N. M.; Morgenstern, A.; Smith, Q. A.; Eberhart, M. E.; Alexandrova, A. N. Histone deacetylase 8: Characterization of physiological divalent metal catalysis. *J. Phys. Chem. B* **2016**, *120*, 5884−95.

(13) Slocum, J. D.; Webb, L. J. Measuring electric fields in biological matter using the vibrational stark effect of nitrile probes. *Annu. Rev. Phys. Chem.* **2018**, *69*, 253−271.

(14) Geng, C.; Li, J.; Weiske, T.; Schlangen, M.; Shaik, S.; Schwarz, H. Electrostatic and charge-induced methane activation by a concerted double C−H bond insertion. *J. Am. Chem. Soc.* **2017**, *139*, 1684−1689.

(15) Chantarojsiri, T.; Reath, A. H.; Yang, J. Y. Cationic charges leading to an inverse free-energy relationship for N-N bond formation by mn(vi) nitrides. *Angew. Chem., Int. Ed. Engl.* **2018**, *57*, 14037−14042.

(16) First, J. T.; Novelli, E. T.; Webb, L. J. Beyond pka: Experiments and simulations of nitrile vibrational probes in staphylococcal nuclease show the importance of local interactions. *J. Phys. Chem. B* **2020**, *124*, 3387−3399.

(17) Jermusek, F. A., Jr.; Webb, L. J. Electrostatic impact of brefeldin a on thiocyanate probes surrounding the interface of arf1-bfa-arno4m, a protein−drug−protein complex. *Biochemistry* **2024**, *63*, 27−41.

(18) Marlton, S. J. P.; McKinnon, B. I.; Hill, N. S.; Coote, M. L.; Trevitt, A. J. Electrostatically tuning the photodissociation of the irgacure 2959 photoinitiator in the gas phase by cation binding. *J. Am. Chem. Soc.* **2021**, *143*, 2331−2339.

(19) Reath, A. H.; Ziller, J. W.; Tsay, C.; Ryan, A. J.; Yang, J. Y. Redox potential and electronic structure effects of proximal nonredox active cations in cobalt schiff base complexes. *Inorg. Chem.* **2017**, *56*, 3713−3718.

(20) Kang, K.; Fuller, J.; Reath, A. H.; Ziller, J. W.; Alexandrova, A. N.; Yang, J. Y. Installation of internal electric fields by non-redox active cations in transition metal complexes. *Chem. Sci.* **2019**, *10*, 10135−10142.

(21) Jo, H.; Culik, R. M.; Korendovych, I. V.; Degrado, W. F.; Gai, F. Selective incorporation of nitrile-based infrared probes into proteins via cysteine alkylation. *Biochemistry* **2010**, *49*, 10354−10356.

(22) Zhang, S.; Zhang, Y.; Ma, X.; Lu, L.; He, Y.; Deng, Y. Benzonitrile as a probe of local environment in ionic liquids. *J. Phys. Chem. B* **2013**, *117*, 2764−2772.

(23) Fried, S. D.; Boxer, S. G. Measuring electric fields and noncovalent interactions using the vibrational stark effect. *Acc. Chem. Res.* **2015**, *48*, 998−1006.

(24) Deb, P.; Haldar, T.; Kashid, S. M.; Banerjee, S.; Chakrabarty, S.; Bagchi, S. Correlating nitrile IR frequencies to local electrostatics quantifies noncovalent interactions of peptides and proteins. *J. Phys. Chem. B* **2016**, *120*, 4034−4046.

(25) Sorenson, S. A.; Patrow, J. G.; Dawlaty, J. M. Solvation reaction field at the interface measured by vibrational sum frequency generation spectroscopy. *J. Am. Chem. Soc.* **2017**, *139*, 2369−2378.

(26) Sarkar, S.; Patrow, J. G.; Voegtle, M. J.; Pennathur, A. K.; Dawlaty, J. M. Electrodes as polarizing functional groups: correlation between hammett parameters and electrochemical polarization. *J. Phys. Chem. C* **2019**, *123*, 4926−4937.

(27) Sarkar, S.; Maitra, A.; Banerjee, S.; Thoi, V. S.; Dawlaty, J. M. Electric fields at metal−surfactant interfaces: A combined vibrational spectroscopy and capacitance study. *J. Phys. Chem. B* **2020**, *124*, 1311−1321.

(28) Zhang, Y.; Ouyang, Y.; Luo, Z.; Dong, S. Convenient, column chromatography-free, and effective synthesis of benzo-21-crown-7 and its derivatives. *Eur. J. Org. Chem.* **2019**, *2019*, 4741−4744.

(29) Wolk, A. B.; Leavitt, C. M.; Garand, E.; Johnson, M. A. Cryogenic ion chemistry and spectroscopy. *Acc. Chem. Res.* **2014**, *47*, 202−210.

(30) Grimme, S. Exploration of chemical compound, conformer, and reaction space with meta-dynamics simulations based on tight-binding quantum chemical calculations. *J. Chem. Theory Comput.* **2019**, *15*, 2847−2862.

(31) Pracht, P.; Bohle, F.; Grimme, S. Automated exploration of the low-energy chemical space with fast quantum chemical methods. *Phys. Chem. Chem. Phys.* **2020**, *22*, 7169−7192.
(32) Becke, A. D. Density-functional thermochemistry. Iii. The role of exact exchange. *J. Chem. Phys.* **1993**, *98*, 5648−5652.
(33) Grimme, S.; Antony, J.; Ehrlich, S.; Krieg, H. A consistent and accurate ab initio parametrization of density functional dispersion correction (dft-d) for the 94 elements h-pu. *J. Chem. Phys.* **2010**, *132*, 154104.
(34) Ditchfield, R.; Hehre, W. J.; Pople, J. A. Self-consistent molecular-orbital methods. Ix. An extended gaussian-type basis for molecular-orbital studies of organic molecules. *J. Chem. Phys.* **1971**, *54*, 724−728.
(35) Hehre, W. J.; Ditchfield, R.; Pople, J. A. Self—consistent molecular orbital methods. Xii. Further extensions of gaussian—type basis sets for use in molecular orbital studies of organic molecules. *J. Chem. Phys.* **1972**, *56*, 2257−2261.
(36) Hariharan, P. C.; Pople, J. A. The influence of polarization functions on molecular orbital hydrogenation energies. *Theor. Chim. Acta* **1973**, *28*, 213−222.
(37) Francl, M. M.; Pietro, W. J.; Hehre, W. J.; Binkley, J. S.; Gordon, M. S.; DeFrees, D. J.; Pople, J. A. Self-consistent molecular orbital methods. Xxiii. A polarization-type basis set for second-row elements. *J. Chem. Phys.* **1982**, *77*, 3654−3665.
(38) Clark, T.; Chandrasekhar, J.; Spitznagel, G. W.; Schleyer, P. V. R. Efficient diffuse function-augmented basis sets for anion calculations. Iii. The 3-21+g basis set for first-row elements, li−f. *J. Comput. Chem.* **1983**, *4*, 294−301.
(39) Frisch, M. J.; Pople, J. A.; Binkley, J. S. Self-consistent molecular orbital methods 25. Supplementary functions for gaussian basis sets. *J. Chem. Phys.* **1984**, *80*, 3265−3269.
(40) Hay, P. J.; Wadt, W. R. Ab initio effective core potentials for molecular calculations. Potentials for k to au including the outermost core orbitals. *J. Chem. Phys.* **1985**, *82*, 299−310.
(41) Hay, P. J.; Wadt, W. R. Ab initio effective core potentials for molecular calculations. Potentials for the transition metal atoms sc to hg. *J. Chem. Phys.* **1985**, *82*, 270−283.
(42) Wadt, W. R.; Hay, P. J. Ab initio effective core potentials for molecular calculations. Potentials for main group elements na to bi. *J. Chem. Phys.* **1985**, *82*, 284−298.
(43) Pierotti, R. A. A scaled particle theory of aqueous and nonaqueous solutions. *Chem. Rev.* **1976**, *76*, 717−726.
(44) Floris, F. M.; Tomasi, J.; Ahuir, J. L. P. Dispersion and repulsion contributions to the solvation energy: Refinements to a simple computational model in the continuum approximation. *J. Comput. Chem.* **1991**, *12*, 784−791.
(45) Cossi, M.; Rega, N.; Scalmani, G.; Barone, V. Energies, structures, and electronic properties of molecules in solution with the c-pcm solvation model. *J. Comput. Chem.* **2003**, *24*, 669−681.
(46) Frisch, M. J.; Trucks, G. W.; Schlegel, H. B.; Scuseria, G. E.; Robb, M. A.; Cheeseman, J. R.; Scalmani, G.; Barone, V.; Petersson, G. A.; Nakatsuji, H., et al. *Gaussian 16*, rev. C.01; Wallingford, CT, 2016.
(47) Sarkar, S.; Tseng, C.; Maitra, A.; Voegtle, M. J.; Dawlaty, J. M. Advances in vibrational stark shift spectroscopy for measuring interfacial electric fields. In Emerging trends in chemical applications of lasers. *American Chemical Society* **2021**, *1398*, 199−224.
(48) Maitra, A.; Das, P.; Thompson, B. C.; Dawlaty, J. M. Distinguishing between the electrostatic effects and explicit ion interactions in a stark probe. *J. Phys. Chem. B* **2023**, *127*, 2511−2520.
(49) Dereka, B.; Lewis, N. H. C.; Keim, J. H.; Snyder, S. A.; Tokmakoff, A. Characterization of acetonitrile isotopologues as vibrational probes of electrolytes. *J. Phys. Chem. B* **2022**, *126*, 278−291.
(50) Foster, a. J.; Weinhold, F. Natural hybrid orbitals. *J. Am. Chem. Soc.* **1980**, *102*, 7211.
(51) Reed, A. E.; Weinhold, F. Natural bond orbital analysis of near-hartree−fock water dimer. *J. Chem. Phys.* **1983**, *78*, 4066.
(52) Reed, A. E.; Weinstock, R. B.; Weinhold, F. Natural population analysis. *J. Chem. Phys.* **1985**, *83*, 735−746.
(53) Reed, A. E.; Weinhold, F. Natural localized molecular orbitals. *J. Chem. Phys.* **1985**, *83*, 1736−1740.
(54) Carpenter, J. E.; Weinhold, F. Analysis of the geometry of the hydroxymethyl radical by the "different hybrids for different spins" natural bond orbital procedure. *Journal of Molecular Structure: THEOCHEM* **1988**, *169*, 41−62.
(55) Reed, A. E.; Curtiss, L. A.; Weinhold, F. Intermolecular interactions from a natural bond orbital, donor-acceptor viewpoint. *Chem. Rev.* **1988**, *88*, 899.
(56) Bagchi, S.; Fried, S. D.; Boxer, S. G. A solvatochromic model calibrates nitriles' vibrational frequencies to electrostatic fields. *J. Am. Chem. Soc.* **2012**, *134*, 10373.

https://doi.org/10.1021/acs.jpclett.4c01303
J. Phys. Chem. Lett. 2024, 15, 7458−7465